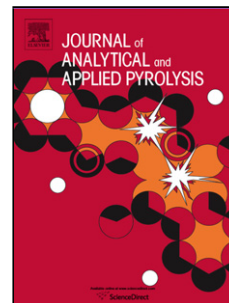


# Journal Pre-proof

How to trace back an unknown production temperature of biochar from chemical characterization methods in a feedstock independent way

Dilani Rathnayake (Investigation) (Writing - original draft), Przemyslaw Maziarka (Formal analysis), Stef Ghysels (Methodology) (Formal analysis), Ondřej Mašek (Resources) (Writing - review and editing) (Supervision), Saran Sohi (Writing - review and editing), Frederik Ronsse (Conceptualization) (Writing - review and editing) (Supervision) (Funding acquisition)



PII: S0165-2370(20)30583-0  
DOI: <https://doi.org/10.1016/j.jaap.2020.104926>  
Reference: JAAP 104926  
To appear in: *Journal of Analytical and Applied Pyrolysis*  
Received Date: 2 August 2020  
Revised Date: 16 September 2020  
Accepted Date: 19 September 2020

Please cite this article as: Rathnayake D, Maziarka P, Ghysels S, Mašek O, Sohi S, Ronsse F, How to trace back an unknown production temperature of biochar from chemical characterization methods in a feedstock independent way, *Journal of Analytical and Applied Pyrolysis* (2020), doi: <https://doi.org/10.1016/j.jaap.2020.104926>

This is a PDF file of an article that has undergone enhancements after acceptance, such as the addition of a cover page and metadata, and formatting for readability, but it is not yet the definitive version of record. This version will undergo additional copyediting, typesetting and review before it is published in its final form, but we are providing this version to give early visibility of the article. Please note that, during the production process, errors may be discovered which could affect the content, and all legal disclaimers that apply to the journal pertain.

© 2020 Published by Elsevier.

## **How to trace back an unknown production temperature of biochar from chemical characterization methods in a feedstock independent way**

Dilani Rathnayake <sup>a1</sup>, Przemyslaw Maziarka <sup>a1</sup>, Stef Ghysels <sup>a</sup>, Ondřej Mašek <sup>b</sup>, Saran Sohi <sup>b</sup>, Frederik Ronsse <sup>a\*</sup>

<sup>a</sup>Thermochemical Conversion of Biomass Research Group, Department of Green Chemistry and Technology, Faculty of Bioscience Engineering, Ghent University, Coupure Links 653, 9000, Ghent, Belgium.

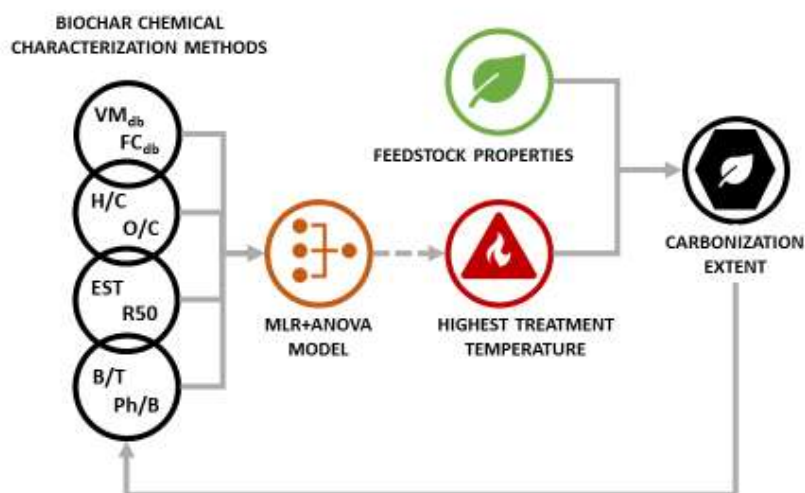
<sup>b</sup>UK Biochar Research Centre, School of GeoSciences, University of Edinburgh, Alexander Crum Brown Road, Edinburgh, EH9 3FF, United Kingdom.

\*Corresponding author email and full postal address: Frederik.Ronsse@UGent.be

Thermochemical Conversion of Biomass Research Group Department of Green Chemistry and Technology, Faculty of Bioscience Engineering, Ghent University, Coupure Links 653, 9000, Ghent, Belgium

<sup>1</sup>These authors share co-first authorship

### **Graphical abstract**



## Highlights

- 24 biochar samples from 12 different feedstocks were characterised using five different chemical characterization methods
- Five feedstock independent indicators were identified based on the principal component analysis
- The highest treatment temperature was modelled using three feedstock-independent indicators
- The multilinear model and auxiliary correlations were positively validated with external datasets

## Abstract

Besides the feedstock composition, the highest treatment temperature (HTT) in pyrolysis is one of the key production parameters. The latter determines the feedstock's carbonization extent, which influences physicochemical properties of the resulting biochar, and in consequence its performance in industrial and agricultural applications. The actual HTT of biomass is difficult to measure in a reliable manner in many large-scale pyrolysis units (e.g., rotary kilns). Therefore, producers and end-users often rely on unreliable or biased information regarding this key production parameter that affects biochar quality. Data from indirect chemical assessment methods of biochar's carbonization extent correlate well with the highest treatment temperature. Therefore, this study demonstrates that the HTT can be accurately assessed *a posteriori* and feedstock-independently via a simple-to-use model based on biochar characteristics related to the carbonization extent. For that purpose, 24 contrasting biochars from 12 different feedstocks produced in the most common production temperature range of 350-700 °C were analysed using 5 different established biochar chemical characterization methods. Then, experimental data was used to establish a multilinear regression model capable of correlating the HTT, which was successfully validated for external datasets. The correlation accuracy for biochars of various origin (lignocellulosic, manure) was satisfactorily high ( $R^2_{adj.} = 0.853$ , RSME = 47 °C). The obtained correlation proved that the HTT can be predicted feedstock independently with the use of basic input data. It also provides a quick, simple, and reliable tool to verify the HTT of a given biochar.

## Key words

Highest treatment temperature, Biochar, Carbonization level, Multilinear correlation, Feedstock-independent parameters

## Abbreviations

HTT	Highest Treatment Temperature
db	Dry basis
daf	Dry ash free basis
Æ	Edinburgh Stability Tool
B	Benzene
T	Toluene
Ph	Phenol
EtB	Ethyl benzene
R50	Recalcitrance index
PCA	Principle Component Analysis
PC	Principle Component
MLR	Multilinear regression
ANOVA	Analysis of variance
RSME	Root Mean Square Error
MAE	Mean Absolute Error

## 1. Introduction

Biochar is the solid, carbon-rich product obtained through pyrolysis of biomass, typically being forestry and agricultural residues or wastes [1]. The production and application of biochar is increasingly gaining interest worldwide. The properties of biochar mainly dictate its possible applications and strongly depend on the carbonization level, which is governed by the feedstock and pyrolysis process conditions used during its production [2]. Several studies have shown a significant correlation between the HTT and biochar's composition (e.g., carbon content, H/C and O/C molar ratio) as well as its structural properties (e.g., BET surface area, micropore volume and surface functionality) [3,4]. Although these features generally correlate with the HTT, significant scattering in the correlations remains due to the feedstock dependence of mentioned parameters.

The effect of feedstock-dependent features on the biochar's structural organisation is harder to predict and to control than the influence of production-dependent features, such as the HTT. In laboratory-scale biochar production, the HTT can theoretically be measured adequately, if multiple thermocouple are in place at various positions. Yet, this is however not always the case, as betimes a set reactor temperature is reported, rather than an actually measured temperature inside a biomass bed. Moreover, the HTT during industrial scale biochar production can vary from the one put forth by the producers. Indeed, the actual production temperature not always reaches the desired pyrolysis temperature along with the HTT (i.e. in between batches or in continuous pyrolysis reactors). The variation in the moisture content of the used feedstock or temperature gradient inside the reactor can be identified as main contributors for that discrepancy. The endothermicity/ exothermicity of the pyrolysis reactions (i.e. its endo or exothermal nature) which can shift the actual HTT in case of conversion of large particles, also contributes to that discrepancy. Moreover, the biochar HTT of different suppliers provided as "production temperature" can also be measured ambiguously (ex-bed, in-bed, etc.) or might be not measured at all (i.e. in simple kilns). Finally, in some instances, a biochar applier may be offered biochar whose production history details not or incompletely known. Since the properties of biochar can be strongly feedstock-dependent, inferring the extent of carbonization without acknowledging this feedstock-dependency can be insufficient or biased. In consequence, it can lead to non-optimal modification or use of biochar in consecutive processes.

The biochar structure contains aromatic rings with different degree of aromatization, which is related to the overall carbonization. The aromaticity of biochar has been found to be strongly dependent on (i) feedstock-dependent features and (ii) production-dependent features [5–10]. The specific influence of the feedstock-dependent features is complex and appears randomised. Nevertheless, some general trends are apparent from literature. Biochar derived from a lignin-rich feedstock (i.e. wood and its residues) tends to reach higher aromaticity, compared to

biochar from mineral-rich feedstocks (i.e. crop residues and processed waste materials like manures and sewage sludge) obtained under the same processing conditions [5–10]. The impact of production-dependent parameters, especially the HTT in pyrolysis on the aromaticity and extent of charring is more comprehensible. It is well known that upon increasing the HTT, a progressive elimination of heteroatoms (through dehydration, decarbonylation and decarboxylation reactions) occurs [11], along with rearrangements (i.e. poly-condensation reactions) in the carbonaceous structure that promote the formation of (poly)aromatic clusters [8,12,13]. Moreover, an increase in temperature increases the degree of aromatic condensation (i.e. the cluster size and the purity of the aromatic structure) as observed through  $^{13}\text{C}$  NMR spectroscopy [8,14,15]. As a result, biochar obtained at higher HTT features particular levels in the aromaticity and degree of aromatic condensation which are not observed in biochar produced at a lower temperature [8]. Unfortunately, the  $^{13}\text{C}$  NMR spectroscopy analysis method, despite its accuracy and reliability, requires expensive instruments, which additionally are not straightforward to use. Therefore, relatively simple and low-cost biochar chemical characterization methods were pursued and introduced, whose role is to indirectly assess the carbonization level of biochar in a less accurate, yet less time-cost expensive manner.

The simplest and most frequently used ones are based on the elemental and proximate analysis, such as H/C molar ratio or fixed carbon content (FC) on a dry basis [16]. Considering that the most stable carbonaceous material is anthracite/graphite with a very well-developed structural organisation and whose H/C is very low and with a FC content close to 100%, other carbonaceous materials can be ranked according to their carbonization level in relation to these reference materials. The R50 stability proxy is based on a very similar basis [17]. Another, relatively new method is the Edinburg stability tool ( $\mathcal{A}$ ), which assess the resistance to chemical oxidation of biochar C [18]. It assumes that the better-developed structure, i.e. a more aromatic char, is more resistant to mineralisation, hence more stable. More complex chemical indicators



are the ones obtained via analytical pyrolysis (Py-GC/MS), such as the benzene to toluene ratio (B/T ratio). Analytical pyrolysis methods are based on the assumption that more recalcitrant carbonaceous structures release less oxygenated or branched aliphatic compounds, as these compounds should already have been released upon the actual char production process. As it can be noticed, all the mentioned biochar characterization methods are indirectly related with the carbonaceous material structural organisation (e.g. aromatization and the extent thereof).

Since changes in the degree of aromatic condensation can occur partially feedstock-independently, the HTT could be considered as a basic indicator of the extent of the biochar's aromatization. Therefore, considering a large-scale production, it could be useful to biochar end-users, producers, and certifiers to know the actual temperature in which biomass was converted. The aim of this study is to create a simple-to-use correlation based on easy-to-measure properties of given biochar, which would allow for quick assessment of its HTT after production. For this purpose, this study assesses the feedstock-independent nature of various established biochar characterization methods described in literature via statistical tools like principal component analysis (PCA). Then, the characterization methods are checked in terms of their predictive power and reliability. This study provides a multilinear correlation between selected predictors and HTT. The obtained MLR model is then validated against various external datasets to assess its accuracy and usefulness.

## **2. Materials and methods**

### **2.1. Biochar materials**

A set of 24 biochar samples with contrasting properties which are produced using lab-scale biochar production reactors was used. They were produced using 12 different feedstocks at 10 different production temperatures with varying heating rates and residence times. The dataset also contained 8 thermo-sequences (groups of biochars from the same feedstock but produced

at different pyrolysis temperature). An overview of the biochars applied in this study is shown in Table 1. All samples used in this study were supplied by the UK Biochar Research Centre.

## **2.2. Elemental analysis**

The mass fractions of carbon, nitrogen, hydrogen on dry basis (wt.%, db) were determined in triplicate, using a Flash 2000 elemental analyser (ThermoScientific, USA). The samples were pre-dried overnight at 105 °C prior to the elemental analysis. The oxygen mass fraction was calculated by difference.

## **2.3. Proximate analysis**

Proximate analysis of biochars was determined in triplicate using TGA [19]. In brief, the moisture content of biochar was obtained from the mass loss upon heating from 30 °C to 110 °C at a heating rate of 25 °C/min and holding at 110 °C for 10 minutes. The volatile matter content on dry basis was determined from the weight loss upon heating from 110 °C at 25 °C/min to 900 °C and holding at 900 °C for 10 minutes. Moisture and volatile matter content determination were carried out in an inert N<sub>2</sub> atmosphere, with 50 ml/min flow rate. The ash content on dry basis was determined from the weight curve after switching the carrier gas from N<sub>2</sub> to air (same flow rate) and after being kept at 900 °C for 20 minutes. Fixed carbon content on dry basis was obtained by difference.

## **2.4. Thermal recalcitrance index (R50)**

Determination of the R50 index from TGA was done according to the procedure described in Harvey et al. [17]. Measurement was done in duplicate. A 70 µl aluminium crucible was fully filled with ca. 10-15 mg biochar (or ca. 5 mg for low-density biochars). Each sample was then heated from 30 °C to 1000 °C with a heating rate of 10 °C/min under Nitrogen flow rate of 10 ml/min. Resulting TG profiles were corrected for moisture and ash contents and thermal recalcitrance index (R50) was obtained using the following equation:

$$R50 = \frac{T_{50,x}}{T_{50,graphite}} \quad (1)$$

where  $T_{50,x}$  is the temperature at which 50% of the sample mass was oxidized (lost), while  $T_{50,graphite}$  is an external standardization factor and corresponds to the temperature at which 50% of a graphite sample is oxidized ( $T_{50,graphite} = 885$  °C) [17].

## 2.5. Edinburgh stability tool

The Edinburgh stability tool, i.e. accelerated aging of biochar, was performed as described by Cross and Sohi [18]. A quantity of ground and pre-dried (105 °C, overnight) biochar corresponding to ca. 0.1 g of carbon was put into a glass test tube. To the tube was added 7 ml deionized water and 0.01 mol of  $H_2O_2$  technical grade (VWR chemicals, Belgium). Tubes with the oxidizer-biochar suspension were heated to 80 °C to induce thermal oxidation and were kept at 80 °C for 48 hours until the hydrogen peroxide solution was evaporated. Upon drying overnight at 105 °C, mass loss was recorded, and the biochar carbon stability ( $\mathcal{A}$ ) was calculated as:

$$\mathcal{A} (\%) = \frac{Br \times BrC}{Bt \times BtC} \times 100 \quad (2)$$

Where  $Br$  denotes the residual mass of biochar after oxidation,  $BrC$  denotes the mass fraction of carbon (wt. %, db) in the residual biochar after oxidation,  $Bt$  denotes the initial mass of biochar and  $BtC$  denotes the corresponding carbon mass fraction (wt. %, db).

Table 1. Biochar samples along with their corresponding feedstock, feedstock type, pyrolysis process conditions and origin (L – lignocellulosic, M-manure, A – algae, W – waste). Thermosequences are labelled with the same superscripts (N/A-not assessed).

ID	Feedstock	Type [-]	HTT [°C]	Retention time [min]	Heating rate [°C/min]
WP-350 <sup>a</sup>	Wood pellets	L	350	40	5.0
WP-650 <sup>a</sup>	Wood pellets	L	650	10	5.0
SP-350.1 <sup>b</sup>	Straw pellets	L	350	10	5.0
SP-350.2 <sup>b</sup>	Straw pellets	L	350	40	5.0
SP-650.1 <sup>b</sup>	Straw pellets	L	650	10	5.0
SP-650.2 <sup>b</sup>	Straw pellets	L	650	40	5.0
SCG-550 <sup>c</sup>	Spent coffee ground	L	550	20	5.0
SCG-700 <sup>c</sup>	Spent coffee ground	L	700	20	5.0
RH-550	Rice husk	L	550	21	N/A
DX-750	<i>Arundo donax</i>	L	750	21	N/A
DM-300 <sup>d</sup>	Digested manure	M	300	90	11.0
DM-400 <sup>d</sup>	Digested manure	M	400	90	12.5
DM-600 <sup>d</sup>	Digested manure	M	600	90	14.0
BM-500 <sup>e</sup>	Bull manure	M	500	90	13.6
BM-600 <sup>e</sup>	Bull manure	M	600	90	14.0
ALG1-450 <sup>f</sup>	<i>Macrocyntis pyrifera</i>	A	450	20	25.0
ALG2-550 <sup>f</sup>	<i>Ascophyllum nodosum</i>	A	550	20	25.0
FW-300 <sup>g</sup>	Food waste	W	300	90	11.0
FW-400 <sup>g</sup>	Food waste	W	400	90	12.5
FW-500 <sup>g</sup>	Food waste	W	500	90	13.6
SW-700	Slaughterhouse waste	W	700	20	5.0
PMW-300 <sup>h</sup>	Paper mill waste	W	300	90	11.0
PMW-400 <sup>h</sup>	Paper mill waste	W	400	90	12.5
PMW-500 <sup>h</sup>	Paper mill waste	W	500	90	13.6

## 2.6. Pyrolysis-GC-MS analysis

Micro-pyrolysis experiments of biochar were performed using a micro-pyrolysis unit (Multi-shot pyrolyser EGA/PY-3030D, Frontier Laboratories Ltd.) coupled to a gas chromatograph (Thermo Fisher Scientific Trace GC) - mass spectrometer (Thermo ISQ MS). Samples were analysed according to the procedure described in Suarez-Abelenda et al. [20]. In brief, ca. 0.5 mg of finely ground and well homogenized biochar sample was loaded into a sample cup, which

afterwards was dropped into a deactivated stainless-steel pyrolysis tube, preheated to 750 °C and kept for 12 seconds. Evolved volatile compounds were swept and separated in a GC (RTX-1701 column, 60 m, 0.25 mm, 0.25 µm, Restek), with an injector temperature of 250 °C and a split ratio of 1:100. Helium was used as a carrier gas (Alphagaz 2-grade helium, Air Liquide) with a constant column flow rate of 1 ml/min. The temperature program of the GC oven, initiated when the sample had been injected was as follows: (a) 3 minutes at constant temperature of 40 °C, (b) heating to 280 °C at 5 °C/min and (c) 1 minute at constant temperature of 280 °C. The GC-separated compounds were identified by a single quadrupole MS with electron ionization with a transfer line temperature of 280 °C and an ion source temperature of 230 °C. The MS was operated with an electron impact ionization of 70 eV and a scan mode between mass-to-charge ratio ( $m/z$ ) values between 45–300, with an acquisition rate of 5 spectra per second. Compounds were identified, based on their retention times and fragmentation patterns, by comparison to the NIST database. Each component concentration was expressed as the component's peak area divided by the total peak area in percent value (rel. area [%]). Ratios between the specific compounds evolved in the Py-GC/MS analysis applied in this study are calculated as the ratio of the relative peak areas of each compound.

## 2.7. Principal component analysis (PCA)

PCA on different datasets was performed in R Studio (3.5.3). A detailed description of the PCA procedure used in this study is provided in the supplementary information (section A). In brief, principal component analysis is a multivariate statistical technique that projects the information contained in a normalised dataset (records, parameters) onto a reduced number of uncorrelated components (dimensions). Typical PCA results in plots of scores and loadings, both on the same, two (i.e. when using two PC's) dimensions that explain most of the variance. The plot of the scores, projected on the new dimensions, visualizes the records (dependent variables) and allows investigating possible similarities or trends within the dataset. The loadings plot provides

information on how certain parameters (independent variables) influence the outcome on the score plot. In the PCA performed in this study, all biochars were considered as the dependent variables, while the independent variables were comprised of all investigated indicators, including the Edinburg stability tool ( $\Delta E$ ), ratios of B/T, B/EtB, Ph/B and Ph/EtB, recalcitrance index (R50), fixed carbon content, volatile matter content, ash content and the atomic H/C and O/C ratios. The latter was done to identify the feedstock independency of the proximate indicators and find those proxies which have strongest correlation to HTT.

## 2.8. Multiple linear regression with analysis of variance

Multiple linear regression (MLR) was applied to obtain correlations between biochar HTT and the biochar carbonization extent indicators based on biochar characterization. MATLAB (9.5) and R Studio (3.5.3) were applied to perform MLR. The detailed procedure of the MLR with analysis of variance (ANOVA) can be found in supplementary information (section A). HTT is one of the most important factors that determines biochar properties (H/C, O/C yield, FC yield) [21]. Next to HTT, biochar properties are also influenced by the retention time, albeit to a lesser extent. However, in small-scale reactors with few heat transfer limitations, Ronsse et al. [22] found no significant differences in elemental and proximate composition in biochars produced with varying retention time (>10 min) once the HTT was 450 °C and above and using lignocellulosic feedstocks. With the exception of the SP-350.1 biochar, all biochars in the dataset being produced at short RT's have been produced at higher temperatures. Hence, the retention time was deemed not significantly influential and as such not included in the model.

The selection of the parameters (indicators based on the characterization methods for carbonization extent) for the temperature prediction model was done by the following sequence. First, indicators' correlations to the production temperature were identified through the determination coefficient ( $R^2$ ). The indicators showing a  $R^2$  value higher than 0.3 were retained as MLR candidate parameters. Moreover, multicollinearity in the dataset was avoided by

considering the variance inflation factor (VIF) test. Parameters with a VIF value above 5 were removed, resulting in the final set of parameters from which MLR+ANOVA analysis started [23,24].

Journal Pre-proof

Table 2. Biochar characterization results: elemental and proximate analysis in wt % and on dry basis (d.b.), elemental ratios in [mol/mol], R50 and  $\Delta E$ . Results presented as average  $\pm$  standard deviation (n=3 for elemental and  $\Delta E$ , n= 2 for proximate analysis and R50)

ID	C [%]	H [%]	N [%]	O [%]	H/C [-]	O/C [-]	Ash [%]	FC [%]	VM [%]	R50 [-]	$\Delta E$ [%]
WP-350	69.0 $\pm$ 2.1	4.8 $\pm$ 0.1	0.1 $\pm$ 0.0	24.6 $\pm$ 2.2	0.8 $\pm$ 0.0	0.3 $\pm$ 0.0	1.4 $\pm$ 0.1	56.7 $\pm$ 1.7	49.7 $\pm$ 1.7	0.6 $\pm$ 0.0	41.7 $\pm$ 1.3
WP-650	84.0 $\pm$ 2.5	2.3 $\pm$ 0.1	0.1 $\pm$ 0.0	11.4 $\pm$ 2.6	0.3 $\pm$ 0.0	0.1 $\pm$ 0.0	2.2 $\pm$ 0.8	83.4 $\pm$ 1.7	12.5 $\pm$ 1.1	0.7 $\pm$ 0.0	84.6 $\pm$ 7.7
SP-350.1	55.0 $\pm$ 1.0	4.6 $\pm$ 0.0	0.8 $\pm$ 0.0	27.9 $\pm$ 0.9	1.0 $\pm$ 0.0	0.4 $\pm$ 0.0	11.7 $\pm$ 0.1	34.3 $\pm$ 0.7	51.5 $\pm$ 1.0	0.5 $\pm$ 0.0	64.2 $\pm$ 8.4
SP-350.2	56.0 $\pm$ 0.1	3.6 $\pm$ 0.0	0.8 $\pm$ 0.0	25.2 $\pm$ 0.1	0.8 $\pm$ 0.0	0.3 $\pm$ 0.0	14.4 $\pm$ 0.3	43.3 $\pm$ 0.4	36.1 $\pm$ 0.4	0.5 $\pm$ 0.0	67.2 $\pm$ 3.2
SP-650.1	64.0 $\pm$ 0.4	1.4 $\pm$ 0.1	0.7 $\pm$ 0.0	19.0 $\pm$ 0.3	0.3 $\pm$ 0.0	0.2 $\pm$ 0.0	14.9 $\pm$ 2.3	48.9 $\pm$ 3.8	29.7 $\pm$ 2.1	0.6 $\pm$ 0.0	98.1 $\pm$ 5.2
SP-650.2	66.0 $\pm$ 0.9	1.2 $\pm$ 0.0	0.6 $\pm$ 0.0	12.3 $\pm$ 0.9	0.2 $\pm$ 0.0	0.1 $\pm$ 0.0	19.9 $\pm$ 0.1	53.6 $\pm$ 0.1	21.4 $\pm$ 0.2	0.6 $\pm$ 0.0	95.6 $\pm$ 5.5
SCG-550	74.0 $\pm$ 0.1	2.7 $\pm$ 0.1	3.7 $\pm$ 0.0	16.4 $\pm$ 0.1	0.4 $\pm$ 0.0	0.2 $\pm$ 0.0	3.2 $\pm$ 0.7	67.8 $\pm$ 1.0	21.9 $\pm$ 1.2	0.6 $\pm$ 0.0	83.1 $\pm$ 0.0
SCG-700	78.0 $\pm$ 1.7	1.1 $\pm$ 1.0	2.8 $\pm$ 0.2	13.0 $\pm$ 2.8	0.2 $\pm$ 0.0	0.1 $\pm$ 0.0	5.1 $\pm$ 0.0	75.6 $\pm$ 0.1	13.8 $\pm$ 0.2	0.6 $\pm$ 0.0	92.5 $\pm$ 10.4
RH-550	45.6 $\pm$ 0.0	1.1 $\pm$ 1.0	0.4 $\pm$ 0.1	12.9 $\pm$ 3.5	0.2 $\pm$ 0.0	0.2 $\pm$ 0.1	39.9 $\pm$ 0.0	48.5 $\pm$ 0.2	11.8 $\pm$ 0.0	0.6 $\pm$ 0.0	64.0 $\pm$ 0.0
DX-750	71.0 $\pm$ 0.1	0.9 $\pm$ 0.0	0.4 $\pm$ 0.0	8.6 $\pm$ 0.1	0.2 $\pm$ 0.0	0.1 $\pm$ 0.0	19.1 $\pm$ 1.1	61.3 $\pm$ 1.8	14.0 $\pm$ 1.6	0.6 $\pm$ 0.0	94.1 $\pm$ 0.2
DM-300	56.0 $\pm$ 0.7	2.9 $\pm$ 0.3	1.9 $\pm$ 0.1	25.2 $\pm$ 0.6	0.6 $\pm$ 0.1	0.3 $\pm$ 0.0	14.0 $\pm$ 0.8	44.3 $\pm$ 0.1	37.3 $\pm$ 1.2	0.5 $\pm$ 0.1	34.8 $\pm$ 1.7
DM-400	64.0 $\pm$ 0.6	2.1 $\pm$ 0.0	1.1 $\pm$ 0.0	18.7 $\pm$ 0.6	0.4 $\pm$ 0.0	0.2 $\pm$ 0.0	14.1 $\pm$ 1.0	53.7 $\pm$ 0.3	28.0 $\pm$ 1.3	0.5 $\pm$ 0.0	78.0 $\pm$ 2.2
DM-600	62.0 $\pm$ 1.5	4.1 $\pm$ 0.2	2.5 $\pm$ 0.0	12.9 $\pm$ 1.2	0.8 $\pm$ 0.0	0.2 $\pm$ 0.0	18.4 $\pm$ 1.9	55.1 $\pm$ 3.0	22.2 $\pm$ 1.6	0.5 $\pm$ 0.0	85.4 $\pm$ 3.4
BM-500	74.0 $\pm$ 0.7	2.8 $\pm$ 0.0	0.2 $\pm$ 0.4	16.1 $\pm$ 1.0	0.5 $\pm$ 0.0	0.2 $\pm$ 0.0	6.9 $\pm$ 1.6	65.0 $\pm$ 2.2	23.3 $\pm$ 3.3	0.5 $\pm$ 0.0	82.2 $\pm$ 2.3
BM-600	76.0 $\pm$ 1.0	0.4 $\pm$ 0.4	0.0 $\pm$ 0.0	16.4 $\pm$ 1.2	0.1 $\pm$ 0.0	0.2 $\pm$ 0.0	7.2 $\pm$ 1.7	67.7 $\pm$ 2.5	20.2 $\pm$ 2.5	0.5 $\pm$ 0.0	87.4 $\pm$ 0.4
ALG1-450	42.0 $\pm$ 0.3	1.9 $\pm$ 0.1	2.4 $\pm$ 0.0	26.8 $\pm$ 0.4	0.6 $\pm$ 0.0	0.5 $\pm$ 0.0	26.9 $\pm$ 0.2	18.8 $\pm$ 1.0	46.3 $\pm$ 0.5	0.5 $\pm$ 0.0	82.3 $\pm$ 1.9
ALG2-550	46.0 $\pm$ 0.1	1.8 $\pm$ 0.0	2.2 $\pm$ 0.0	16.7 $\pm$ 0.1	0.5 $\pm$ 0.0	0.3 $\pm$ 0.0	33.3 $\pm$ 0.5	22.0 $\pm$ 0.1	38.4 $\pm$ 0.5	0.6 $\pm$ 0.0	88.5 $\pm$ 0.0
FW-300	65.0 $\pm$ 2.3	6.9 $\pm$ 0.3	4.6 $\pm$ 0.3	11.3 $\pm$ 2.9	1.3 $\pm$ 0.0	0.1 $\pm$ 0.0	12.3 $\pm$ 0.7	32.3 $\pm$ 1.1	52.9 $\pm$ 0.2	0.4 $\pm$ 0.0	38.7 $\pm$ 3.5
FW-400	57.0 $\pm$ 1.1	2.6 $\pm$ 0.0	4.6 $\pm$ 0.9	11.8 $\pm$ 1.9	0.6 $\pm$ 0.0	0.2 $\pm$ 0.0	24.0 $\pm$ 0.1	39.2 $\pm$ 0.1	33.3 $\pm$ 0.0	0.6 $\pm$ 0.0	52.6 $\pm$ 6.8
FW-500	55.0 $\pm$ 0.8	2.9 $\pm$ 0.0	3.9 $\pm$ 0.4	16.6 $\pm$ 1.1	0.6 $\pm$ 0.0	0.2 $\pm$ 0.0	21.7 $\pm$ 2.4	47.0 $\pm$ 2.8	28.0 $\pm$ 1.0	0.6 $\pm$ 0.0	82.5 $\pm$ 3.2
SW-700	62.0 $\pm$ 0.0	1.5 $\pm$ 0.1	8.9 $\pm$ 0.4	13.1 $\pm$ 2.7	0.3 $\pm$ 0.0	0.2 $\pm$ 0.1	14.5 $\pm$ 1.1	67.9 $\pm$ 1.5	12.0 $\pm$ 0.4	0.9 $\pm$ 0.0	66.4 $\pm$ 3.3
PMW-300	21.0 $\pm$ 1.0	1.2 $\pm$ 1.3	0.1 $\pm$ 0.0	32.4 $\pm$ 0.7	0.7 $\pm$ 0.0	1.2 $\pm$ 0.1	45.4 $\pm$ 0.6	3.7 $\pm$ 0.0	51.0 $\pm$ 0.6	0.5 $\pm$ 0.0	43.0 $\pm$ 0.5
PMW-400	20.0 $\pm$ 0.2	2.2 $\pm$ 0.1	0.2 $\pm$ 0.0	25.7 $\pm$ 0.3	1.3 $\pm$ 0.0	1.0 $\pm$ 0.0	51.9 $\pm$ 2.5	3.1 $\pm$ 0.5	44.9 $\pm$ 1.9	0.5 $\pm$ 0.0	53.0 $\pm$ 1.6
PMW-500	19.0 $\pm$ 0.1	0.5 $\pm$ 0.0	0.0 $\pm$ 0.0	25.4 $\pm$ 0.1	0.3 $\pm$ 0.0	1.0 $\pm$ 0.0	55.1 $\pm$ 0.4	4.4 $\pm$ 0.2	40.3 $\pm$ 0.4	0.5 $\pm$ 0.0	56.0 $\pm$ 1.0



MLR+ANOVA of the chosen carbonization extent indicators was performed to correlate to the (known) production temperature. The procedure of eliminating each parameter that was statistically irrelevant for the correlation had been repeated multiple times via a looping procedure. It was performed until all parameters that remained after elimination, fulfilled the statistical t-test. In other words, after the elimination procedure, the MLR equation contained the minimum number of indicators based on biochar characterization which were necessary to correctly predict the production temperature. The final correlation between production temperature and selected biochar carbonization extent indicators was validated against external datasets obtained from literature to prove the correlation's reliability and usefulness.

### **3. Results and discussion**

Results from the elemental and proximate analysis, thermal recalcitrance index (R50) and Edinburgh stability tool ( $\Delta E$ ) measurements are presented in Table 2.

#### **3.1. Elemental and proximate analysis**

Results of elemental and proximate analysis showed a significant difference between the biochar samples tested. The same typically observed trends with increasing pyrolysis temperature, such as relative C enrichment, increase in FC content and reduction of VM content, were observed in the studied thermo-sequences (Table 2), especially for biochar produced from lignocellulosic feedstock. Figure 1 shows a van Krevelen diagram of the investigated samples, with indication of proposed International Biochar Initiative (IBI) and European Biochar Certificate (EBC) limits ( $\leq 0.7 \text{ H/C}_{\text{org}}$  and  $\leq 0.4 \text{ O/C}$ ) for stable biochar [16,25]. According to the IBI and EBC guidelines, it is recommended to do an acid treatment prior to organic C determination in order to avoid the impact from inorganic carbon species [16,25], but this acid treatment was not applied in this study. The data in Figure 1 is presented with the assumption that all C from elemental analysis can be considered as organic C. Figure 1 indicates that 9 out of 24 samples (of which 4 produced above 350 °C) do not meet the EBC

requirements.

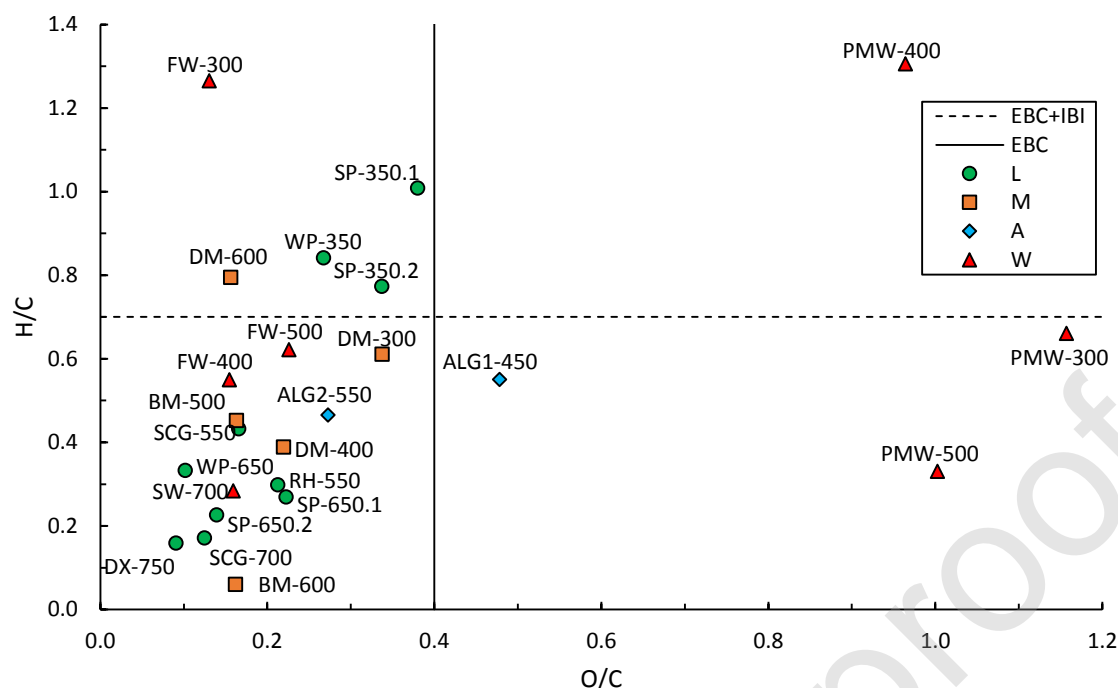


Figure 1. Van Krevelen diagram of investigated biochar samples with EBC and IBI limits for H/C and O/C molar ratios, respectively [16,25]

Therefore, those samples cannot be considered as full-fledged biochar. Moreover, 3 samples originating from paper mill waste (PMW) stand out as clear outliers. From the results of the proximate analysis, those samples also stand out due to their very low fixed carbon content (<5%) and ash content exceeding 50%.

### 3.2. Thermal recalcitrance index (R50)

Harvey et al. proposed a classification of biochar's C sequestration ability based on the R50 value [17]. That classification states that an  $R50 > 0.7$  indicates high biochar carbonization extent (i.e., high stability),  $0.5 < R50 < 0.7$  represents an intermediate stability and  $R50 < 0.5$  indicates a low biochar stability. In this context, only SW-700 had a high ability to sequester carbon. SP-300, PMW-400, PMW-500, DM-300, FW-300, ALG1-450 had a lower C

sequestration ability and all the other biochar samples had an intermediate capacity to sequester C in soil.

### 3.3. Edinburgh stability tool ( $\Delta E$ )

The Edinburgh stability tool ( $\Delta E$ ) depicts the oxidative degradation of biochar in soil. Moreover, it can be used as a proxy for the environmental aging of approximately 100 years under temperate conditions [18]. According to Crombie et al. [26] the stable carbon fraction in biochar increases with the biochar production temperature due to the elimination of the volatile fraction. Results of the Edinburgh stability tool in this study (Table 2) showed that its values differed significantly among the biochars from the different feedstocks, even at the same production temperature. On the other hand, the values of the  $\Delta E$  within 7 out of the 8 thermo-sequences showed a clear trend. Coefficient of determination between  $\Delta E$  and production temperature was high for biochars derived from lignocellulosic biomass ( $R^2=0.74$ ) compared to biochar derived from waste and algae feedstocks ( $R^2=0.41$ ). This may be due to the heterogeneity of the waste and algae feedstock materials compared to the lignocellulosic biomass.

### 3.4. Py-GC/MS analysis

Analytical pyrolysis allows thermal degradation of the compounds under inert atmosphere [27]. Hence, it provides information regarding the biomolecular composition of chars [28]. Pyrolysis product ratios obtained through Py-GC/MS analysis is shown in Table 3. Typically, benzene, toluene, ethylbenzene, PAHs, and phenols are predominantly presented in pyrograms of biochar [29,30]. Therefore, these compounds and their homologues with alkyl side chains can be transformed into ratios. Next, they can be used as an indicator of the degree of thermal alteration and dealkylation in the pyrolysis products [20,27]. Due to the significant thermal stability of the char produced at high HTT, their pyrograms are characterized with fewer pyrolysis products out of which benzene is the predominant one [28,31,32].

Table 3. Ratios of relative peak areas of selected compounds based on Py-GC/MS analysis (B – benzene, T – toluene, Ph – phenol and EtB – ethylbenzene)

ID	B/T	B/EtB	Ph/B	EtB/Ph
[Unit]	[-]	[-]	[-]	[-]
WP-350	0.8	4.6	2.0	9.5
WP-650	3.2	13.3	0.0	0.1
SP-350.1	0.9	4.7	0.7	3.2
SP-350.2	1.2	7.5	0.2	1.3
SP-650.1	4.3	34.5	0.0	0.0
SP-650.2	2.3	8.0	0.0	0.0
SCG-550	2.7	50.3	0.0	0.0
SCG-700	3.2	24.8	0.0	0.3
RH-550	3.4	17.8	0.2	4.2
DX-750	3.5	7.6	0.1	0.6
DM-300	0.8	5.1	0.8	3.8
DM-400	1.6	8.2	0.3	2.4
DM-600	2.2	16.9	0.2	2.9
BM-500	1.9	15.0	0.1	1.1
BM-600	3.5	14.8	0.1	1.3
ALG1-450	1.9	19.4	0.0	0.4
ALG2-550	3.0	9.6	0.0	0.2
FW-300	1.1	3.8	0.2	0.9
FW-400	1.5	5.7	0.1	0.7
FW-500	1.4	7.8	0.1	0.8
SW-700	3.8	12.3	0.0	0.3
PMW-300	1.3	5.4	0.7	3.5
PMW-400	1.1	9.8	0.3	2.9
PMW-500	2.1	14.0	0.1	1.4

Therefore, the B/T ratio derived from Py-GC/MS analysis was used as an indicator to assess carbonization level of biochar in several studies and showed a good correlation with the biochar HTT [20,27,29,30]. In this study as well, the B/T ratio of biochars showed a good positive correlation with the biochar HTT ( $R^2 = 0.78$ ). However, it is not that much stronger as previously reported [20,27,29,30]. This may be due to the diversity of the biochar feedstock material used in this study. Suarez-Abelenda et al. [20] reported that biochars from N rich, hence protein-rich feedstocks produced at low temperatures are able to introduce bias into the measured B/T ratio via the addition of toluene derived from incompletely converted protein, especially the amino acid phenylalanine produces toluene upon pyrolysis. Moreover, in this

study Ph/B, B/EtB, EtB/Ph ratios were used to examine their correlation with biochar HTT. Phenol tends to be increasingly released from chars treated between 400 °C to 800 °C due to demethoxylation of methoxyphenols (as decomposition products from lignin) and starts to decrease at 800 °C because of phenol dehydroxylation [27]. However, none of these ratios showed strong correlation with biochar HTT.

### 3.5. PCA on combined indicators derived through biochar characterization

PCA was conducted to see the relationship between production temperature and different biochar characterization indicators associated with biochar's carbonization level.  $C_{daf}$ , H/C and O/C molar ratios, ash, volatile matter (VM), and fixed C content (FC) from elemental and proximate analysis were selected as the independent variables for PCA. Indicators from elemental and proximate analysis were used and expressed on dry basis, unless specified otherwise.

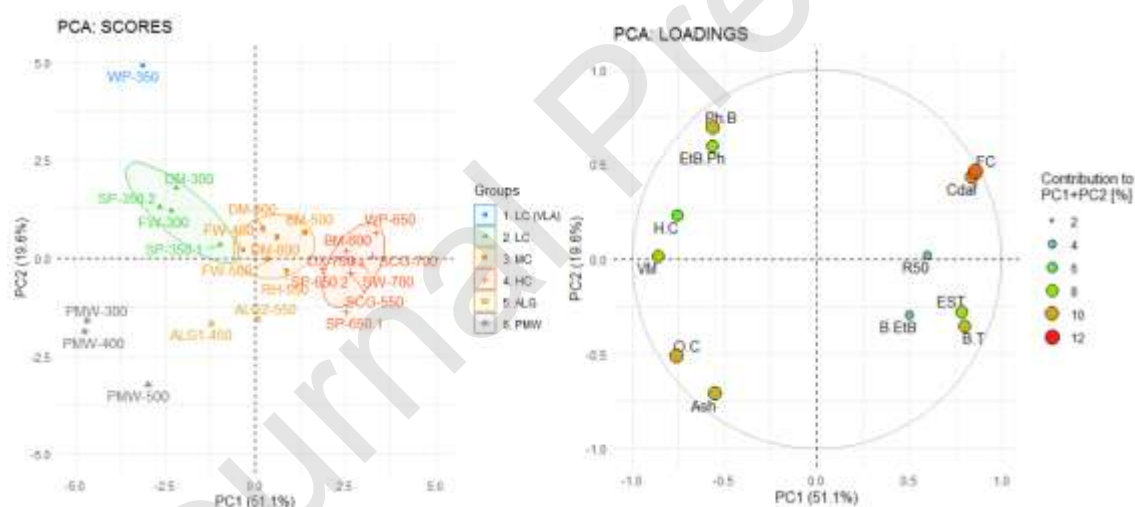


Figure 2. Scores (left) and loadings (right) plot from PCA performed on a dataset with all measured data. (LC – low carbonization, MC – medium carbonization, HC – high carbonization, VLA – very low ash content, ALG – biochar from algal feedstock, PMW – biochar from paper mill wastes, EST- Edinburgh stability tool (Æ)).

Although the ash content could be assumed as a feedstock-dependent parameter, it had been retained in the PCA due its tendency to increase in concentration with material conversion. Also, both the R50 and  $\bar{A}$  indicators as well as the B/T, B/EtB, Ph/B and Ph/EtB ratios obtained from Py-GC/MS were included in the PCA.

The scores and loadings plot from the PCA are shown in Figure 2. The application of different indicators based on biochar characterization as parameters led to high explained variance via first two PCs. PC1 accounted for 51.1%, while the PC2 accounted for 19.6%, which gave in total 70.7% of the total variance explained (above the threshold of 70%). As presented on the scores plot in Figure 2 (left), most of the records are located in close proximity. However, some outliers like PMW or WP-350 are also visible. A general and important observation of the score plot is that the biochar sample points are self-organized, based on the severity of the production parameters, hence the carbonization extent or organization of their structure. The biochar sample points were visually organized into 3 clusters: LC – low carbonized, MC – medium carbonized and HC – highly carbonized regarding to their presumed extent of structural organization.

The location of parameters and their contribution to the principal components on the loadings plot in Figure 2 (right) explain the alignment of the biochar samples on the score plot. Indicators, whose high value is usually linked to low production temperature (VM, H/C and O/C), were located on the negative end of the PC1 axis. Indicators with a significant extent of structural organization ( $C_{daf}$ , FC, B/T) were located on the positive side of axis of PC1, together with indicators such as R50 and  $\bar{A}$ . Therefore, elevated values for the indicators ( $C_{daf}$ , FC, B/T, R50 and  $\bar{A}$ ) can be related to high HTT and presumed elevated biochar aromatization. Biochar samples organize according to the conversion severity (scores plot) by changes in the biochar carbonization extent indicators (loading plot). This supports the existence of a correlation between the HTT and the biochar's structural organization as indicated by the proxy methods.

Information on the loading plot gives evidence that PC1 can be constrained to the HTT of the investigated biochar samples. Parameters like the phenol/ethylbenzene peak area ratio and ash content had the lowest contribution to PC1 (supplementary information, section B) leading to the conclusion that they are less relevant to this dimension (i.e. production temperature).

Although PC2 explains only a modest c.a. 20% of the total variance, useful insights were drawn on its basis. Highest contributors to PC2 are the ash content and Py-GC/MS ratios with phenol, which carried virtually no information on the biochar's structural organization extent. The lowest contributions were by VM content, R50, H/C and  $\Delta E$ , which carried a lot of information on the HTT. Biochars on the higher end and lower ends of PC2 in the score plot were produced at a lower production temperature (PMW samples - high in ash, and WP-350 - high in phenol). At lower temperature, the role of the feedstock type dominates the placement of biochar in the PCA more than the HTT.

Altogether the PCA suggests that PC1 and PC2 are rather complementary, with PC1 explaining variance induced by the severity of the conversion including the HTT and PC2 explaining variance induced by the feedstock-dependency. The trajectory of several thermosequences, like both SP thermosequences (SP-350 to SP-650), also illustrates that a positive increase on PC1 (HTT) is observed, as well as a positive increase on PC2 (feedstock feature, in this case content of ash).

### **3.6. Assessment of temperature predictors**

#### **3.6.1. Analysis of predictive power**

For the quantitative assessment of the predictive power of the parameters (i.e., carbonization extent indicators) with respect to the highest treatment temperature, PMW samples were not considered, as these were obvious outliers as indicated by the van Krevelen chart (Figure 1) as well as the PCA score plot (Figure 2). The complete dataset without outliers was subdivided

into 3 groups, depending on the feedstock used for biochar production: lignocellulosic (L), manure (M) and waste + algae (W+A). The result from correlation analysis between the HTT and all the predictors and detailed results of the temperature-predictor correlation analysis for each feedstock group can be found in supplementary information, section C).

The correlation analysis between the HTT and all the predictors (supplementary information, section C) confirms the results obtained in PCA, with respect to those predictors that contribute to PC1. In general, the higher the positive loading to PC1 for a given predictor, the higher the  $R^2$  in the regression analysis. It is worth mentioning that the determination coefficient of a given predictor for the whole dataset is not the mathematical mean of the determination coefficients of each of the 3 feedstock type groups. This is apparent in the correlation analysis between the HTT and all the predictors (supplementary information, section C) for VM content and EtB/Ph ratio, where the  $R^2$  value for each feedstock group (L, M, W+A) indicates greater correlation to HTT than in the overall dataset ('All' in the correlation analysis between the HTT and all the predictors (supplementary information, section C). Moreover it shows that correlations built with only one feedstock group can induce significant bias in case of its application on a given sample outside of the feedstock group, leading to secondary feedstock-dependency.

With the aim to build a multilinear model to correlate HTT to biochar carbonization extent indicators, only those predictors that showed a feedstock-independent correlation were retained. Hence, a threshold value of 0.3 for the determination coefficient ( $R^2$ ) between predictor for the whole dataset and production temperature was set. The threshold translates to an absolute Pearson correlation coefficient of  $>0.5$  (existence of a correlation). As a result, ash content, Py-GC/MS ratios of Ph/B, EtB/Ph and B/EtB were no longer retained as HTT predictors. These predictors also correspond to those which explained low variance for PC1 and high variance for PC2 in PCA.



### 3.6.2. Analysis of repeatability and reliability of R50, $\text{AE}$ and B/T ratio

Since the results of the elemental and proximate analysis had been proven through numerous publications to be consistent and reliable [26,33], these predictors do not require additional analysis and can be retained in the construction of a multilinear regression model further on. The more complex, and less common indicators such as R50,  $\text{AE}$  and B/T ratio require additional checking to confirm that they are consistent among different datasets.

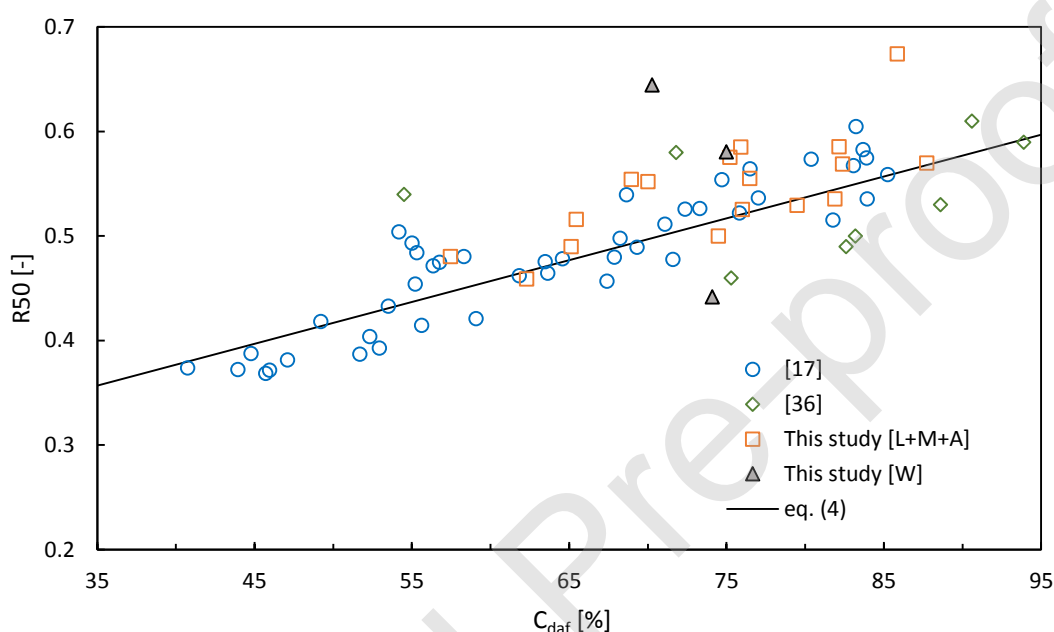


Figure 3. Comparison between R50 data from this study and literature sources calculated using the correlation presented in eq. (4).

The mentioned indicators were mutually correlated with other feedstock-independent predictors, using external data. By doing so, (i) it was assessed which predictors were not biased by the applied methodology, hence, which were reliable and repeatable and (ii) correlations were obtained to replace these complex predictors.

In the comprehensive review of Klasson [33], a correlation between R50 and  $C_{daf}$  had been introduced as shown in eq. (4).

$$R50 = 0.217 + 0.004 C_{daf} \quad (4)$$

The correlation was built on experimental data of lignocellulosic biochar from Harvey et al. [17], which summarise the data from other authors [10,34,35]. Figure 3 shows experimental data from this study, along with data from Windeatt et al. and Harvey et al. [17,36] with the correlation proposed by Klasson [33]. Almost all experimental data points from this study are consistent with the literature sources (Figure 3). It shows that biochars from this study having a certain  $C_{daf}$  showed the same R50 comparable with literature data. It proves that R50 can be used as a reliable and repeatable predictor. Additionally, it can be stated that the correlation provided by Klasson [33] is stable ( $R^2$  for 3 different datasets = 0.72) and can be applied for biochar originating from lignocellulosic, manure and algae biomass.

In the work of Klasson, (2017) [33] is also presented a correlation between the  $\Delta E$  and molar O/C ratio, shown in eq. (5). This correlation had been established using the data of lignocellulosic biochars from Crombie et al. [26]. Figure 4 shows experimental data from this study and from Crombie et al. [26] with the correlation proposed by Klasson [33].

$$\Delta E = (1 - 2.24 O/C) \quad (5)$$

As Figure 4 indicates, only biochar samples from lignocellulosic biomass (L) and manure (M) show similarity in trend and values in comparison to data from Crombie et al. [26], unlike waste (W) and algae (A) derived biochars. This is in line with the results presented in the correlation analysis between the HTT and all the predictors (supplementary information, section C), in which the correlation of the production temperature to the O/C ratio and  $\Delta E$  for waste and algae derived biochar was assessed to be very weak to virtually none.

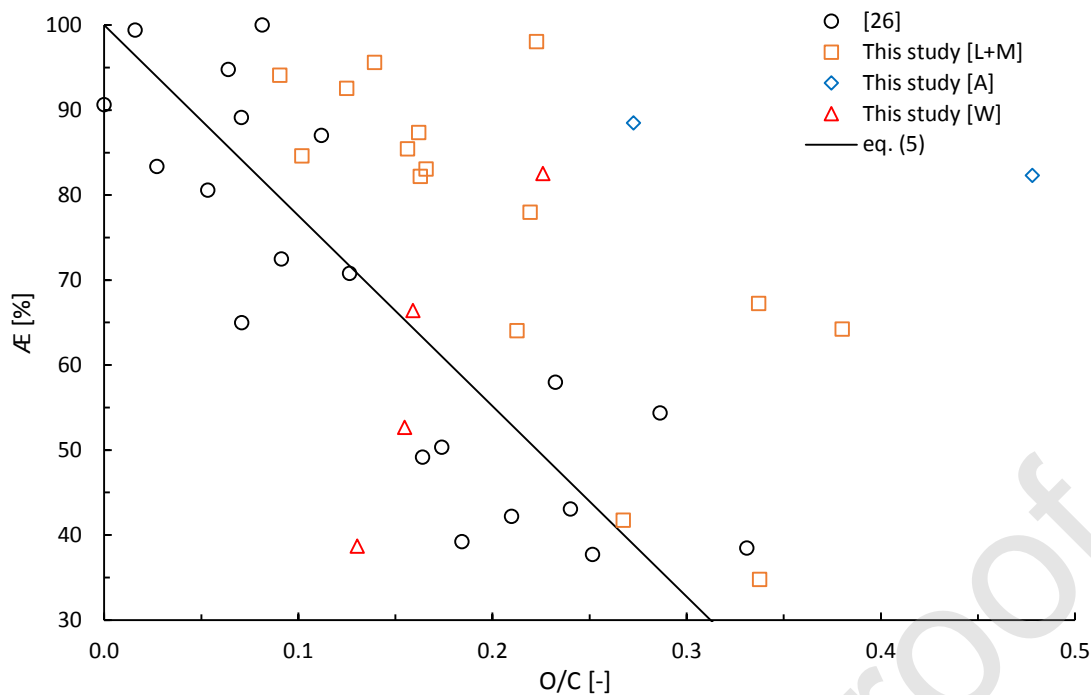


Figure 4. Comparison between  $\bar{A}E$  data from this study and data from Crombie et al. [26] with the correlation presented in eq. (5).

Use of the  $\bar{A}E$  as predictor is therefore only reliable and repeatable for the L and M derived biochars. When merging the L+M datasets, the accuracy of eq. (5) is getting lower ( $R^2 = 0.542$ ) and there is a tendency to underpredict the  $\bar{A}E$  value. Nevertheless, the correlation is still satisfactory, and that parameter showed acceptable accuracy and reproducibility.

The last complex predictor investigated in this assessment is the B/T ratio, originating from Py-GC/MS data. In literature reports [28,32,37], the B/T value of biochar can be found, but only few have been obtained with the same analytical procedure. Since the Py-GC/MS method is very sensitive to measurement conditions, only data from similar procedures can be compared. Figure 5 compares this study's B/T ratio and literature data obtained using the same procedure. It is worth mentioning that Kaal et al. and Pereira et al. [28,29] only used lignocellulosic derived biochars, but Suarez-Abelenda et al. [20] included manure and algae derived biochars in their dataset.

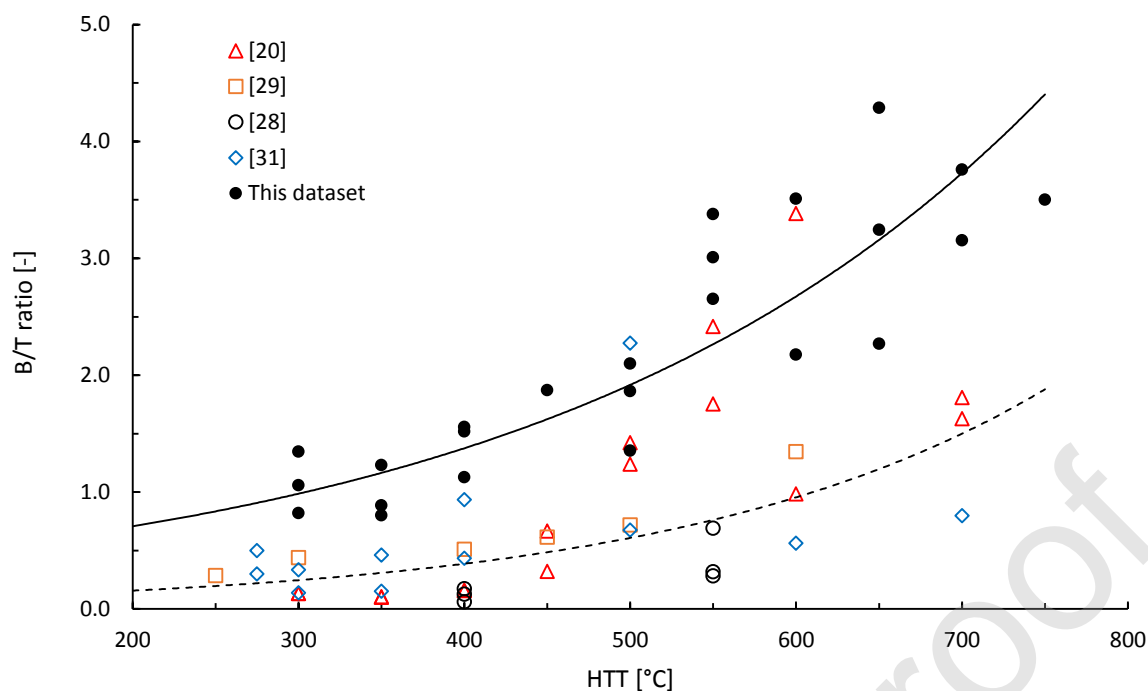


Figure 5. Comparison between B/T ratio data from this study and literature sources.

As Figure 5 shows, the B/T ratios in this study are for every HTT, on average, several times higher than those from the literature sources. This is most likely due to the different analytical instruments used. The B/T ratios from the works of other studies consider here [20,28,29,31] were obtained on the Pyroprobe series 5000 (CDS analytics) pyrolyzer connected to an HP-5MS polysiloxane-based (non-polar) separation column. The difference in the pyrolysis setups between the mentioned researches and this study could cause differences in heating rate and vapour residence times in the reactor zone as well in the transfer line. Presumably this may have influenced the obtained pyrograms, especially through increasing of the secondary cracking reactions that can occur, if the heating rate is not high enough or if vapour residence times in the heated zones are prolonged (heat-mass transfer limitation) [38]. Additionally, the difference in the column polarity could lead to the higher selectivity for different compounds among studies, i.e. higher detection of the shorter hydrocarbons in case of the application of non-polar columns.

Closer data analysis indicates that the results from this study and literature show similar trends with the treatment temperature, albeit with different magnitude. The best fit between B/T ratio and HTT is obtained through an exponential function. Hence, it can be concluded that the B/T ratio suffers from two major issues. One is being the poor reproducibility in terms of using different analytical setups; the second is being the non-linearity. Therefore, its incorporation into a multilinear model would be in contradiction to the principles of linear model construction. For this reason, it was decided not to retain the B/T ratio in the selected set of the temperature predictors for the MLR.

### **3.7. Multilinear model for prediction of biochar's production temperature**

#### **3.7.1. Model calibration**

The initial predictors that were accurate, reliable, and repeatable were retained, being:  $C_{daf}$ , H/C, O/C,  $FC_{db}$ ,  $VM_{db}$ , R50 and  $\Delta E$ . The training dataset consisted of the 21 biochars, as mentioned in section 3.6.1. Application of the MLR+ANOVA procedure on the dataset of initial predictors, resulted in temperature-predictors based correlation (model) with 3 final predictors: O/C, R50 and  $\Delta E$ . All other predictors showed strong multicollinearity ( $5 < VIF$ ) or their strength of variance was not significant ( $t\text{-test} > t^*$ ). The statistical features (estimate, p-value, etc.) of the predictors of the HTT correlation, summarized information regarding temperature prediction model and its overall performance on the training dataset and residual analysis of the model is presented in supplementary information.

Despite the inhomogeneous input dataset, the model showed a  $R^2$  adj. higher than 0.85 and a root mean squared error (RSME) lower than 50 °C. Among the predictors, the  $\Delta E$  had the strongest relative influence (>50%) on the predicted outcome. An accurate measurement of the  $\Delta E$  value is therefore likely to result in a higher accuracy of prediction of production temperature (supplementary information, section D).

### 3.7.2. Model validation

To prove the model's reliability and usefulness, it was validated against literature data. However, no literature datasets were found that contained simultaneously both  $R_{50}$  and  $\Delta E$  values. Therefore, datasets with the missing parameters were completed using the appropriate auxiliary equations (section 3.6.2). It needs to be emphasized that all the production temperatures, specified in literature, are regarded as the HTT, despite the lack of complete certainty of it and possible introduction of a random error to the model's prediction.

For a first validation of the MLR model, data from lignocellulosic biochars from Crombie et al. [26] was used, containing experimental values of the  $\Delta E$ . The value of the  $R_{50}$  (which was not present in the original dataset) used for validation was calculated from eq. (4). The validation results are presented in supplementary information (section E). The obtained value of the  $R^2$  is 0.843 and of the RSME is 63°C. The model very accurately predicted the HTT for pine wood derived biochar, and a moderate accuracy for rice husk and wheat straw derived biochar was obtained, presumably to the higher ash content found in those biochars.

Another validation was performed against combined data [39–44] summarised by Klasson [33]. The validation dataset contained data of biochars derived from lignocellulosic (L), manure and manure mixed with lignocellulosic biomass (M). This dataset lacked values of  $R_{50}$  and  $\Delta E$ , which for validation purposes were calculated using eq. (4) and eq. (5). The validation results and residuals are presented in supplementary information (section E and F). Considering that the model's predictions were solely based on data from elemental and proximate analysis, the overall model performance is more than satisfactory. The accuracy of HTT prediction for lignocellulosic derived biochars was slightly higher than for manure and the mixture dataset. This was likely due to the greater share of lignocellulosic derived biochars in the training dataset. The model predicts the HTT in the range between 350 °C and 700 °C with the highest accuracy, but still a small over-estimation is noticed in the middle of the mentioned range.

Results also show rapid accuracy loss beyond both ends of the range. It is strongly related with the training dataset's temperature range, which did not contain samples produced below 350 °C and only one sample produced above 700 °C (Figure 6).

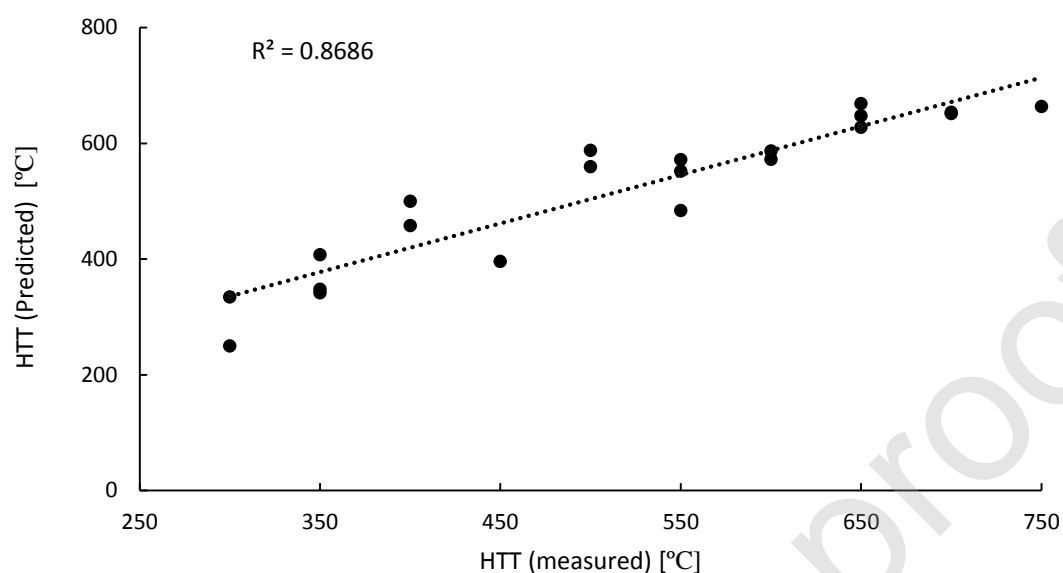


Figure 6. Comparison between measured HTT and predicted HTT.

### 3.7.3. Model summary

The summarised outcome of both model validations is presented in Table 4.

Table 4. Summarized outcome of the validation against different datasets from literature

Feedstock	Predictors			Results			Validation data source
	O/C	R50	Æ	R <sup>2</sup>	MAE (°C)	RSME (°C)	
Lignocellulosic	exp.	calc.	exp.	0.843	53	65	[26]
All	exp.	calc.	calc.	0.708	61	78	[39–44]
Lignocellulosic (L)	exp.	calc.	calc.	0.720	58	74	
Manure + mix (M)	exp.	calc.	calc.	0.681	67	84	

From validation, it can be concluded that, even for datasets which lacked the experimental data (such as Æ or R50), the predicted HTT is satisfactorily accurate. It implies that the obtained





foundation laid by this study can help in consecutive investigation of feedstock-independent correlations between the HTT and the overall biochar's carbonization extent. This study gives evidence that the HTT, the parameter most influential to biochar's carbonization, hence composition and structural properties, despite strong variability in the feedstock, can be accurately assessed through established correlations. It can be stated that the obtained simple-to-use correlation constitutes a useful tool for quick and fairly accurate verification of the HTT of biochars produced at a large-scale. With the use of the correlation, it is possible to not only predict the actual carbonization extent of the obtained biochar but also investigate if the production installation works with the optimal thermal regime.

#### Author Credit Statement

**Dilani Rathnayake:** Investigation, Writing - Original Draft. **Przemysław Maziarka:** Formal analysis. **Stef Ghysels:** Methodology, Formal analysis. **Ondřej Mašek:** Resources, Writing - Review & Editing, Supervision. **Saran Sohi** Writing - Review & Editing. **Frederik Ronsse:** Conceptualization, Writing - Review & Editing, Supervision, Funding acquisition

#### Declaration of interests

☒ The authors declare that they have no known competing financial interests or personal relationships that could have appeared to influence the work reported in this paper.

#### Acknowledgement

This study received funding from the European Union's Horizon 2020 research and innovation programme under the Marie Skłodowska-Curie grant agreement No 721991. Also, we would like to acknowledge Christian Wurzer at UK Biochar Research Centre for his support during thermogravimetric analysis.

## References

- [1] S. Shackley, S. Sohi, An assessment of the benefits and issues associated with the application of biochar to soil., 2010. [https://www.geos.ed.ac.uk/homes/sshackle/SP0576\\_final\\_report.pdf](https://www.geos.ed.ac.uk/homes/sshackle/SP0576_final_report.pdf).
- [2] J. Wang, Z. Xiong, Y. Kuzyakov, Biochar stability in soil: Meta-analysis of decomposition and priming effects, *GCB Bioenergy*. 8 (2016) 512–523. doi:10.1111/gcbb.12266.
- [3] A.R. Zimmerman, B. Gao, M.Y. Ahn, Positive and negative carbon mineralization priming effects among a variety of biochar-amended soils, *Soil Biol. Biochem.* 43 (2011) 1169–1179. doi:10.1016/j.soilbio.2011.02.005.
- [4] K. Weber, P. Quicker, Properties of biochar, *Fuel*. 217 (2018) 240–261. doi:10.1016/J.FUEL.2017.12.054.
- [5] J.A. Baldock, R.J. Smernik, Chemical composition and bioavailability of thermally altered *Pinus resinosa* ( Red pine ) wood, *Org. Geochem.* 33 (2002) 1093–1109.
- [6] M. Keiluweit, P.S. Nico, M.G. Johnson, Dynamic Molecular Structure of Plant Biomass-Derived Black Carbon ( Biochar ), *Environ. Sci. Technol.* 44 (2010) 1247–1253.
- [7] A. V. McBeath, R.J. Smernik, M.P.W. Schneider, M.W.I. Schmidt, E.L. Plant, Determination of the aromaticity and the degree of aromatic condensation of a thermosequence of wood charcoal using NMR, *Org. Geochem.* 42 (2011) 1194–1202.

doi:10.1016/j.orggeochem.2011.08.008.

- [8] A. V Mcbeath, R.J. Smernik, E.S. Krull, J. Lehmann, The influence of feedstock and production temperature on biochar carbon chemistry : A solid-state  $^{13}\text{C}$  NMR study, *Biomass and Bioenergy*. 60 (2013) 121–129. doi:10.1016/j.biombioe.2013.11.002.
- [9] B.P. Singh, A.L. Cowie, R.J. Smernik, Biochar Carbon Stability in a Clayey Soil As a Function of Feedstock and Pyrolysis Temperature, *Environ. Sci. Technol.* (2012). doi:10.1021/es302545b.
- [10] A.R. Zimmerman, W. Hall, P.O. Box, Abiotic and Microbial Oxidation of Laboratory-Produced Black Carbon ( Biochar ), *Environ. Sci. Technol.* 44 (2010) 1295–1301.
- [11] F. Ronsse, R.W. Nachenius, W. Prins, Carbonization of Biomass, in: *Recent Adv. Thermo-Chemical Convers. Biomass*, 2015: pp. 293–324.
- [12] J. Bourke, M. Manley-harris, C. Fushimi, K. Dowaki, T. Nunoura, M.J. Antal, Do All Carbonized Charcoals Have the Same Chemical Structure ? 2 . A Model of the Chemical Structure of Carbonized Charcoal, *Ind. Eng. Chem. Res.* (2007) 5954–5967. doi:10.1021/ie070415u.
- [13] K. Nishimiya, T. Hata, Y. Imamura, S. Ishihara, Analysis of chemical structure of wood charcoal by X-ray photoelectron spectroscopy, *J. Wood Sci.* (1998) 56–61.
- [14] D. Chen, X. Yu, C. Song, X. Pang, J. Huang, Y. Li, Effect of pyrolysis temperature on the chemical oxidation stability of bamboo biochar, *Bioresour. Technol.* 218 (2016) 1303–1306. doi:10.1016/j.biortech.2016.07.112.
- [15] W.C. Hockaday, S. Joseph, C.A. Masiello, Temperature Sensitivity of Black Carbon Decomposition and Oxidation, 44 (2010) 3324–3331.
- [16] A. Budai, A.R. Zimmerman, A.L. Cowie, J.B.W. Webber, B.P. Singh, B. Glaser, C.A.

- Masiello, Biochar Carbon Stability Test Method: An assessment of methods to determine biochar carbon stability, (2013).
- [17] O.R. Harvey, L. Kuo, A.R. Zimmerman, P. Louchouart, J.E. Amonette, B.E. Herbert, An Index-Based Approach to Assessing Recalcitrance and Soil Carbon Sequestration Potential of Engineered Black Carbons (Biochars), *Environ. Sci. Technol.* (2012). doi:10.1021/es2040398.
- [18] A. Cross, S.P. Sohi, A method for screening the relative long-term stability of biochar, *GCB Bioenergy*. 5 (2013) 215–220. doi:10.1111/gcbb.12035.
- [19] W. Buss, O. Masek, Mobile organic compounds in biochar e A potential source of contamination e Phytotoxic effects on cress seed ( *Lepidium sativum* ) germination, *J. Environ. Manage.* 137 (2014) 111–119. doi:10.1016/j.jenvman.2014.01.045.
- [20] M. Suarez-Abelenda, J. Kaal, A. McBeath, Translating analytical pyrolysis fingerprints to Thermal Stability Indices (TSI) to improve biochar characterization by pyrolysis-GC-MS, *Biomass and Bioenergy*. 98 (2017) 306–320. doi:10.1016/j.biombioe.2017.01.021.
- [21] S. Ghysels, F. Ronsse, D. Dickinson, W. Prins, Production and characterization of slow pyrolysis biochar from lignin-rich digested stillage from lignocellulosic ethanol production, *Biomass and Bioenergy*. 122 (2019) 349–360. doi:10.1016/j.biombioe.2019.01.040.
- [22] F. Ronsse, S. Van Hecke, D. Dickinson, W. Prins, Production and characterization of slow pyrolysis biochar: influence of feedstock type and pyrolysis conditions, *Gcb Bioenergy*. 5 (2013) 104–115. doi:10.1111/gcbb.12018.
- [23] M.H. Kutner, C. Nachtsheim, J. Neter, *Applied linear regression models*, 4th ed., McGraw-Hill/Irwin, 2004., 2004.

- [24] S. Sheather, A modern approach to regression with R, Springer Science & Business Media, 2009. doi:10.1007/978-0-387-09608-7.
- [25] H. Schmidt, T. Bucheli, C. Kammann, B. Glaser, S. Abiven, J. Leifeld, European Biochar Certificate—Guidelines for a Sustainable Production of Biochar, 2016.
- [26] K. Crombie, O. Mašek, S.P. Sohi, P. Brownsort, A. Cross, The effect of pyrolysis conditions on biochar stability as determined by three methods, GCB Bioenergy. 5 (2013) 122–131. doi:10.1111/gcbb.12030.
- [27] J. Kaal, C. Rumpel, Can pyrolysis-GC / MS be used to estimate the degree of thermal alteration of black carbon ?, Org. Geochem. 40 (2009) 1179–1187. doi:10.1016/j.orggeochem.2009.09.002.
- [28] R.C. Pereira, J. Kaal, M.C. Arbestain, R.P. Lorenzo, W. Aitkenhead, M. Hedley, F. Macías, J. Hindmarsh, J.A. Maciá-agulló, Contribution to characterisation of biochar to estimate the labile fraction of carbon, Org. Geochem. 42 (2011) 1331–1342. doi:10.1016/j.orggeochem.2011.09.002.
- [29] J. Kaal, M.P.W. Schneider, M.W.I. Schmidt, Rapid molecular screening of black carbon ( biochar ) thermosequences obtained from chestnut wood and rice straw : A pyrolysis-GC / MS study, Biomass and Bioenergy. 45 (2012) 115–129. doi:10.1016/j.biombioe.2012.05.021.
- [30] R. Conti, D. Fabbri, I. Vassura, L. Ferroni, Comparison of chemical and physical indices of thermal stability of biochars from different biomass by analytical pyrolysis and thermogravimetry, J. Anal. Appl. Pyrolysis. 122 (2016) 160–168. doi:10.1016/j.jaap.2016.10.003.
- [31] J. Kaal, A.M. Cortizas, O. Reyes, M. Soliño, Molecular characterization of Ulex

- europaeus biochar obtained from laboratory heat treatment experiments – A pyrolysis – GC / MS study, J. Anal. Appl. Pyrolysis. 95 (2012) 205–212. doi:10.1016/j.jaap.2012.02.008.
- [32] D. Fabbri, C. Torri, K.A. Spokas, Analytical pyrolysis of synthetic chars derived from biomass with potential agronomic application ( biochar ). Relationships with impacts on microbial carbon dioxide production, J. Anal. Appl. Pyrolysis. 93 (2012) 77–84. doi:10.1016/j.jaap.2011.09.012.
- [33] K.T. Klasson, Biomass and Bioenergy Biochar characterization and a method for estimating biochar quality from proximate analysis results, Biomass and Bioenergy. 96 (2017) 50–58. doi:10.1016/j.biombioe.2016.10.011.
- [34] K. Hammes, R.J. Smernik, J.O. Skjemstad, A. Herzog, U.F. Vogt, M.W.I. Schmidt, Synthesis and characterisation of laboratory-charred grass straw ( *Oryza sativa* ) and chestnut wood ( *Castanea sativa* ) as reference materials for black carbon quantification, Org. Geochem. 37 (2006) 1629–1633. doi:10.1016/j.orggeochem.2006.07.003.
- [35] L. Kuo, B.E. Herbert, P. Louchouart, Can levoglucosan be used to characterize and quantify char / charcoal black carbon in environmental media ?, Org. Geochem. 39 (2008) 1466–1478. doi:10.1016/j.orggeochem.2008.04.026.
- [36] J.H. Windeatt, A.B. Ross, P.T. Williams, P.M. Forster, M.A. Nahil, S. Singh, Characteristics of biochars from crop residues : Potential for carbon sequestration and soil amendment, J. Environ. Manage. 146 (2014) 189–197. doi:10.1016/j.jenvman.2014.08.003.
- [37] J. Kaal, A. V Mcbeath, M. Su, Translating analytical pyrolysis fingerprints to Thermal Stability Indices ( TSI ) to improve biochar characterization by pyrolysis-GC-MS, Biomass and Bioenergy. 98 (2017) 306–320. doi:10.1016/j.biombioe.2017.01.021.

- [38] F. Ronsse, D. Dalluge, W. Prins, R.C. Brown, Optimization of platinum filament micropyrolyzer for studying primary decomposition in cellulose pyrolysis Optimization of platinum filament micropyrolyzer for studying primary decomposition in cellulose pyrolysis, *J. Anal. Appl. Pyrolysis*. 95 (2012) 247–256. doi:10.1016/j.jaap.2012.02.015.
- [39] T. Cordero, F. Marquez, J. Rodriguez-mirasol, J.J. Rodriguez, Predicting heating values of lignocellulosics and carbonaceous materials from proximate analysis, *Fuel*. 80 (2001) 1567–1571.
- [40] P.T. Williams, A.R. Reed, Pre-formed activated carbon matting derived from the pyrolysis of biomass natural fibre textile waste, *J. Anal. Appl. Pyrolysis*. 70 (2003). doi:10.1016/S0165-2370(03)00026-3.
- [41] A. Enders, K. Hanley, T. Whitman, S. Joseph, J. Lehmann, Bioresource Technology Characterization of biochars to evaluate recalcitrance and agronomic performance, *Bioresour. Technol.* 114 (2012) 644–653. doi:10.1016/j.biortech.2012.03.022.
- [42] K.B. Cantrell, P.G. Hunt, M. Uchimiya, J.M. Novak, K.S. Ro, Bioresource Technology Impact of pyrolysis temperature and manure source on physicochemical characteristics of biochar, *Bioresour. Technol.* 107 (2012) 419–428. doi:10.1016/j.biortech.2011.11.084.
- [43] K.B. Cantrell, J.M. Novak, Poultry litter and switchgrass blending for biochar production, *Trans. ASABE*. 57 (2014) 543–553. doi:10.13031/trans.57.10284.
- [44] F. Karaosmanog, A. Isigigur-Ergudenler, S. Aydın, Biochar from the Straw-Stalk of Rapeseed Plant, *Energy & Fuels*. 21 (2000) 336–339. doi:10.1021/ef9901138.